PAPER

Roles of hydroxyl and carbonate radicals in bisphenol a degradation via a nanoscale zero-valent iron/percarbonate system: influencing factors and mechanisms†

Yulun Xiao,[ab] Xiang Liu,[c] Ying Huang,[d] Wei Kang,[e] Zhen Wang[bc] and Han Zheng ⓘ *[b]

In this work, nanoscale-zero-valent iron (nZVI) was applied to activate sodium percarbonate (SPC) to eliminate bisphenol A (BPA), which poses a risk to ecological and human health as a typical endocrine disruptor. The influence of nZVI loading, SPC dosing, initial pH, and the presence of inorganic anions (including Cl^-, HPO_4^{2-}, NO_3^- and NO_2^-) and humic acid on BPA removal by the nZVI/SPC system were investigated. Based on the scavenger test results, $^\bullet OH$ and $CO_3^{\bullet-}$ participated in the degradation of BPA, and $^\bullet OH$ was illustrated to be the dominant radical. The X-ray diffraction (XRD) and X-ray photoelectron spectroscopy (XPS) analysis suggested that surface iron oxide generation, electron transfer and Fe^{2+} release were the main processes of the SPC activation by nZVI. Moreover, BPA transformation products were detected by LC-MS allowing the proposal of a possible degradation pathway of BPA. Along with the degradation of the parent compound BPA, the total organic carbon (TOC) gradually decreased, while the bio-toxicity increased at the initial stage of the reaction (0–3 min) and then decreased to a lower level rapidly at 20 min. Overall, this study evidenced the feasibility of the nZVI/SPC system to efficiently degrade BPA, broadening the applications of nZVI in wastewater treatment.

1. Introduction

In recent decades, bisphenol A (BPA), as a precursor in the manufacture of polycarbonate, epoxy resin and polystyrene,[1] has resulted in the ubiquitous presence of BPA in mineral water bottles, medical equipment and food packaging. Due to the improper disposal and clearance of this BPA-containing waste, BPA is directly or indirectly released into various water bodies.[2,3] It was found that the concentration of BPA in drinking water, surface water and waste landfill leachate could reach 0.1 μg L^{-1}, dozens of μg L^{-1} and 17.2 mg L^{-1}, respectively.[2,4] As a typical endocrine disruptor,[5] BPA poses a risk to aquatic wildlife and human beings even at low concentrations.[6] However, BPA could not be effectively degraded from wastewater by the conventional

strategies including coagulation, filtration, adsorption and biodegradation.[7,8] Therefore, it is urgent to develop an efficient method to abate BPA from water and to simultaneously decrease the bio-toxicity of BPA.

Currently, hydroxyl radical ($^\bullet OH$)-based advanced oxidation processes (AOPs) have been considered as a powerful technology for BPA remediation,[9–11] which is based on the activation of liquid H_2O_2 to generate $^\bullet OH$. In the traditional Fenton system, H_2O_2 could be catalyzed by Fe^{2+} to form $^\bullet OH$ for organic contaminants elimination.[12] But, H_2O_2 was unstable and easily decomposed, making it difficult to transportation and storage.[13,14] Sodium percarbonate (SPC), as the solid phase carrier of H_2O_2, is a promising alternative to liquid H_2O_2 due to the low cost, high stability, and effective activation.[13,15] In addition, the by-products of SPC decomposition contain Na_2CO_3, which can react with $^\bullet OH$ to form carbonate radical (CO_3^-) and accelerate the degradation of contaminants with electron-donating moieties (eqn (1)–(3)).[16,17] Based on these advantages, increasing attentions have been paid to the homogeneous activation of SPC by Fe^{2+}/Fe^{3+}, which has great power in the remediation of organic contaminants in water. Miao et al.[18] demonstrated that perchloroethylene was efficiently oxidized by the Fe^{2+}/SPC system in groundwater, and $^\bullet OH$ was the main active species, showing better performance than the traditional Fenton process at the similar reaction conditions (eqn (4)–(6)). Nevertheless, there are unavoidable

*a*Faculty of Science, Monash University, Clayton, VIC, 3800, Australia

*b*Hubei Key Laboratory of Mine Environmental Pollution Control and Remediation, Hubei Polytechnic University, Huangshi, 435003, China. E-mail: zhenghan@hbpu.edu.cn; Fax: +86-0714-6348286; Tel: +86-0714-6348671

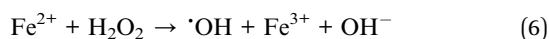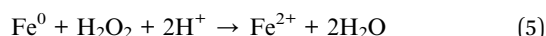*c*School of Environmental Studies, China University of Geosciences, Wuhan 430074, China
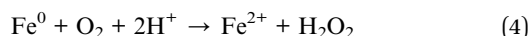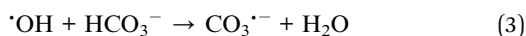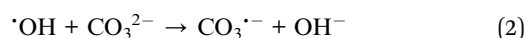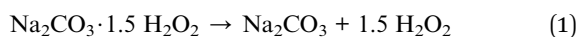
*d*College of Chemical and Biological Engineering, Key Laboratory of Biomass Chemical Engineering of Ministry of Education, Zhejiang University, Hangzhou 310027, China

*e*School of Environmental Science and Engineering, Hubei Polytechnic University, Huangshi, 435003, China

† Electronic supplementary information (ESI) available. See DOI: 10.1039/d0ra08395j

drawbacks such as narrow reaction pH rang, non-recycle of catalyst and precipitation of ferric hydroxide ($Fe(OH)_3$), which results in large amount of iron sludge.[19] In order to overcome these limitations, nanoscale zero-valent iron (nZVI), as an non-toxic, and easy recycled catalyst with relatively large specific surface area, shows excellent potential in activating peroxide oxidants, such as persulfate, peroxymonosulfate, bisulfite and hydrogen peroxide, for removing organic contaminants.[20–24] In the process of nZVI/hydroperoxide, organic pollutants are mainly destroyed by the generated $^{\cdot}OH$ and purified by the Fe^0 corrosion products (iron oxides).[25] However, there have not been any comprehensive mechanistic studies on the activation of SPC by nZVI for the removal of contaminants of emerging concern.

$$Na_2CO_3 \cdot 1.5\ H_2O_2 \rightarrow Na_2CO_3 + 1.5\ H_2O_2 \tag{1}$$

$$^{\cdot}OH + CO_3^{2-} \rightarrow CO_3^{\cdot -} + OH^- \tag{2}$$

$$^{\cdot}OH + HCO_3^- \rightarrow CO_3^{\cdot -} + H_2O \tag{3}$$

$$Fe^0 + O_2 + 2H^+ \rightarrow Fe^{2+} + H_2O_2 \tag{4}$$

$$Fe^0 + H_2O_2 + 2H^+ \rightarrow Fe^{2+} + 2H_2O \tag{5}$$

$$Fe^{2+} + H_2O_2 \rightarrow {}^{\cdot}OH + Fe^{3+} + OH^- \tag{6}$$

Herein, in the present study, it is aimed to investigate the insight of the mechanisms of SPC activation by nZVI for BPA degradation in wastewater. The operation parameters of the nZVI/SPC system were optimized, such as nZVI dosage, SPC concentration, and initial pH. The influences of the nature water constituents on the BPA degradation were carefully evaluated, including the Cl^-, HPO_4^{2-}, NO_2^-, NO_3^- anions, and humic acid (HA). The changes of the chemical compounds on the surface of the pristine and used nZVI were characterized to propose the possible mechanisms for SPC activation. Finally, the transformation products (TPs) were detected to assist the bio-toxicity analysis during the BPA degradation, providing the fundamental knowledge and theoretic support for the future applications of nZVI/SPC method in the wastewater treatment.

2. Materials and methods

2.1 Chemicals

Bisphenol A (BPA, >99.8%), isopropyl alcohol (IPA, ACS, $\geq$ 99.5%) and phenol (PhOH, ACS) were supplied by Aladdin Chemistry. Sodium percarbonate ($Na_2CO_3 \cdot 1.5\ H_2O_2$, SPC, 98%) was purchased from Sigma-Aldrich. Other analytical grade chemicals provided by Sinopharm Chemical Reagent. No further purification was employed for all reagents. The ultrapure water (18.2 Ω cm) was conducted to prepare reagents.

2.2 Preparation of the nZVI catalyst

The nZVI particle was synthesized by the liquid phase reduction method.[26] Detailed process was described in ESI.†

2.3 Catalytic degradation experiments

In this study, unless otherwise noted, all batch experiments were performed at room temperature (25 $\pm$ 2 °C) in 250 mL beaker. The initial concentration of BPA was 0.1 mM and the total volume was 100 mL. Following the addition of a desired amount of SPC, the initial pH of mixture was adjusted with 0.1 M H_2SO_4 as quickly as possible. BPA degradation was initiated by adding certain dosages of nZVI under continuously mechanical agitation. 1.0 mL sample was collected and immediately mixed with 1.0 mL of methanol to quench the residual reactive species at predetermined time intervals. Afterwards, the samples were filtered through 0.22 μm PVDF membranes.

To evaluate the reusability of catalyst, the used nZVI particles were collected by magnetic separation and washed with ultrapure water. Then, the recycled catalysts were utilized for the next reaction under the identified conditions. All the experiments were conducted in triplicate to ensure the accuracy of data.

2.4 Analytical and characterization method

The concentration of BPA was measured using high performance liquid chromatography (HPLC, RIGOL L-3000, China), equipped with a Compass C_{18} column (5 μm, 4.6 $\times$ 250 mm) and UV detector (wavelength at 280 nm for BPA). The mobile phase was consist of acetonitrile and ultrapure water (40 : 60, v/v) with a constant flow rate of 1.0 mL min^{-1}. The injection volume was 20 μL and column temperature was set at 35 °C.

The concentrations of Fe^{2+} ions were colorimetrically measured using the standard method.[27] Briefly, o-phenanthroline was added into the filtered reaction solution and the resulting solution was measured at 510 nm wavelength on a UV-vis light spectrophotometer. The contained Fe^{3+} ions were reduced to Fe^{2+} ions by oxammonium hydrochloride to measure the concentrations of total iron ions in the reaction solutions. Total Organic Carbon (TOC) was determined with a TOC/TN analyzer (multi N/C 2100, Jena, German) to assess the mineralization rate of BPA. The transformation products of BPA were determined by an ultrahigh performance Liquid Chromatography (UPLC, UltiMate 3000, Dionex) coupled with a mass spectrometer (MS, Q-Orbitrap, Thermo Scientific). The UPLC-MS was performed with negative electrospray ionization (ESI$^-$) in a full-scan range of 50–350 m/z at 40 °C. The injection volume was 1 μL. The biological toxicity during the BPA degradation process was evaluated by the activated sludge inhibition test (ASIT) as previously reported.[28]

The structure and crystal phase of nZVI before and after use were analyzed by X-ray diffraction (XRD, D8 Advance, Bruker, Germany) using Cu Kα radiation. The chemical states of Fe and O were analyzed by X-ray photoelectron spectroscopy using monochromatic 100 eV Al-Kα radiation (XPS, ESCALAB 250Xi, Thermo Fisher).

2.5 Kinetics analysis

Based on the BPA removal pattern, the BPA degradation kinetics in nZVI/SPC system should follow a pseudo-first-order reaction, as shown in eqn (7).

$$\ln(C_t/C_0) = -k_{obs}t \qquad (7)$$

Where C_t is the concentration of BPA (mM) at reaction time t (min) and C_0 is the initial BPA concentration (mM), respectively. k_{obs} represents the observed rate constant (min^{-1}).

3.   Results and discussion

3.1   Degradation kinetics of BPA by nZVI/SPC

In this work, various reaction processes were performed to assess the BPA degradation efficiency, including nZVI, SPC, nZVI/SPC, nZVI/H_2O_2 and Fe^{2+}/SPC systems. As shown in Fig. 1, BPA was slightly removed in the presence of nZVI or SPC alone within 20 min. The results indicated that nZVI was ineffective to adsorb molecular BPA (pk_a = 9.6–10.2).[29] Moreover, SPC has limited oxidation ability to remove BPA without activation. When nZVI combined with SPC, BPA was completely removed within 20 min, suggesting that nZVI has an excellent performance on the SPC activation. However, BPA degradation was deceased in the reaction system of nZVI/H_2O_2. Because carbonates from SPC could transform to be $CO_3^{\bullet-}$ through eqn (2) and (3), which favor to oxidize the electron-rich organic pollutants,[13,16,30] resulting in the improvement of BPA degradation efficiency in the nZVI/SPC system.

The chemical stability and reusability of prepared nZVI were evaluated by for its future applications in the wastewater treatment. As shown in the Fig. 2, more than 99% of the BPA was degraded in the first two runs, while about 78% of the BPA was removed in the third run. The catalytic activity of nZVI decreased in the continuous operations, which might be ascribed to two main reasons. The first reason might be the surface corrosion and iron ions dissolution, which reduced the active sites on nZVI. The second one might be the iron ions precipitation products that would deposit on the nZVI surface, hindering the activation of SPC.[31] Overall, these results confirmed that nZVI has a prominent catalytic ability with limited reusability in the nZVI/SPC system.
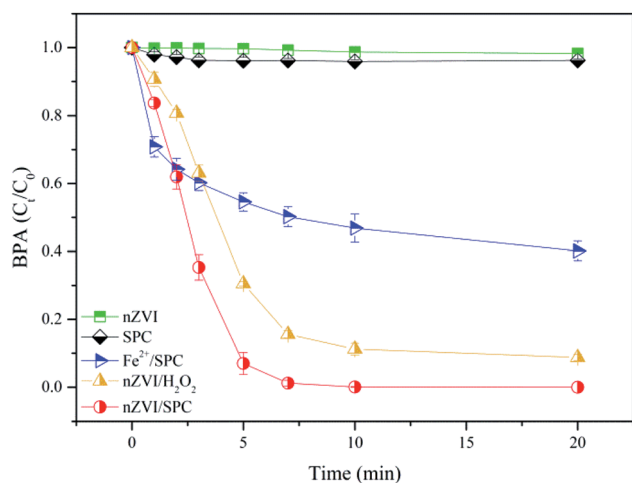

Fig. 2   Reusability of nZVI: $[BPA]_0$ = 0.1 mM, $[nZVI]_0$ = 0.1 g L^{-1}, $[SPC]_0$ = 3 mM, pH_0 = 4.0.

In order to assess the contribution of leached Fe^{2+} from nZVI to the SPC activation in the SPC system, the concentration of dissolved Fe^{2+} was measured and the performance of Fe^{2+}/SPC was compared with nZVI/SPC. As shown in the Fig. 3, the concentration of total Fe (including Fe^{3+} and Fe^{2+} ions) gradually increased to 2.3 mg L^{-1} and then remained relatively stable, which mainly consist of Fe^{2+}. Fe^{3+} could be rapidly reduced to Fe^{2+} by nZVI through eqn (8). Since the surface-associated Fe(II) atoms and dissolved Fe^{2+} ions could also activate H_2O_2 to decompose the organic contaminants,[32,33] 2.3 mg L^{-1} of Fe^{2+} was added with the SPC to evaluate the performance for BPA removal. As shown in Fig. 1, only about 40% of BPA was eliminated in the Fe^{2+}/SPC system, while more than 99% of BPA was removed in the nZVI/SPC system. Unlike homogeneous catalysis, surface active sites of nZVI could promote catalytic oxidation reaction in heterogeneous processes.[33] These results suggested that both heterogeneous and homogeneous catalysis contributed to BPA degradation by nZVI/SPC, but the heterogeneous reactions played a primary role.
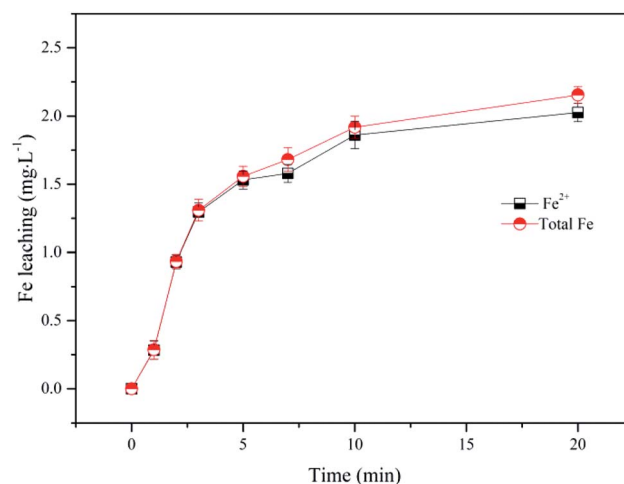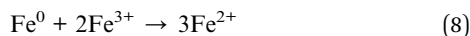

Fig. 1   BPA degradation in various systems. General reaction conditions: $[BPA]_0$ = 0.1 mM, $[nZVI]_0$ = 0.1 g L^{-1}, $[Fe^{2+}]_0$ = 2.3 mg L^{-1}, $[H_2O_2]_0$ = 4.5 mM, $[SPC]_0$ = 3 mM, pH_0 = 4.0.

Fig. 3   Fe leaching in nZVI/SPC system: $[BPA]_0$ = 0.1 mM, $[nZVI]_0$ = 0.1 g L^{-1}, $[SPC]_0$ = 3 mM, and pH_0 = 4.0.

$$Fe^0 + 2Fe^{3+} \rightarrow 3Fe^{2+} \qquad (8)$$

3.2 Effects of operating parameters on BPA degradation

3.2.1 Effects of nZVI loading and SPC dosing on BPA degradation.
To explore the effect of catalyst performance, the degradation efficiency of BPA was investigated at different nZVI dosages from 0.05 g L^{-1} to 0.5 g L^{-1}. As presented in Fig. 4a, BPA removal rate was significantly enhanced with the increase of nZVI dosage from 0.05 g L^{-1} to 0.2 g L^{-1}. Correspondingly, the observed rate constant (k_{obs}) was enhanced from 0.294 min^{-1} to 0.694 min^{-1} (inset in Fig. 4a). More nZVI dosage could provide more active sites for activating SPC, which was conducive to the formation of more free radicals.[34] However, with the further increase of nZVI loading (0.2–0.5 g L^{-1}), BPA removal efficiency was significantly inhibited, as the k_{obs} was reduced (inset in Fig. 4a). It was deduced that excess nZVI would lead to agglomeration, which would reduce the effective collision between nZVI and H$_2$O$_2$;[34,35] Besides, the superabundant Fe^{2+} leached from the excess nZVI might scavenge $^{\bullet}$OH through eqn (9).[24,25,34]

$$Fe^{2+} + {}^{\bullet}OH \rightarrow Fe^{3+} + OH^- \qquad (9)$$
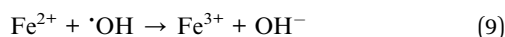
The influence of SPC concentration (0.5 mM, 1 mM, 3 mM and 6 mM) in nZVI/SPC system was studied to evaluate the contribution of oxidant on BPA removal. As illustrated in Fig. 4b, BPA degradation efficiency was enhanced when SPC concentration increased from 0.5 mM to 3 mM. However, BPA degradation was slightly restrained with further increase of SPC dose from 3 mM to 6 mM. Moreover, k_{obs} in nZVI/SPC system exhibited a consistent trend (inset in Fig. 4b). These results revealed that SPC with the moderate concentration was beneficial to form sufficient active species, promoting the elimination of BPA.[19,35] However, excessive H$_2$O$_2$, disaggregated from SPC in the bulk solution, could play as a scavenger of $^{\bullet}$OH or other radicals as shown in eqn (10) and (11),[19,36] causing the decreasing of BPA degradation efficiency.

$$H_2O_2 + {}^{\bullet}OH \rightarrow H_2O + O_2^{\bullet -} + H^+ \qquad (10)$$

$$O_2^{\bullet -} + {}^{\bullet}OH \rightarrow OH^- + O_2 \qquad (11)$$
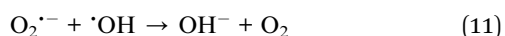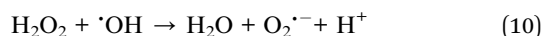
3.2.2 Effect of initial pH on BPA degradation.
According to the previous work,[12] solution pH was a crucial factor in organic pollutants remediation in Fenton or Fenton-like systems. A series of tests were conducted to investigate the effect of initial pH (pH$_0$ at 3.0, 4.0, 5.0 and 6.0) on BPA removal. Fig. 5a showed that BPA oxidation efficiency in nZVI/SPC system was closely related to pH$_0$, implying that BPA degradation was a pH dependent process. It was observed that BPA could be completely removed during 10 min reaction at pH$_0$ = 3.0 and 4.0, especially showing a higher removal rate (85.3%) at the initial reaction (0–1 min). The results were in accordance with the conclusion that acidic pH condition was beneficial to release Fe^{2+} (Fig. 5b), promoting the generation of $^{\bullet}$OH.[37] In contrast, the degradation efficiency of BPA gradually declined with the rise of pH$_0$. For instance, BPA removal rate decreased from 46.0% to 24.1% when the pH$_0$ increased from 5.0 to 6.0. This phenomenon could be explained in three aspects: first, when the solution pH$_0$ increased from 3.0 to 4.0, 5.0 and 6.0, the concentration of Fe^{2+} gradually dropped from 17.80 mg L^{-1} to 2.31 mg L^{-1}, 0.14 mg L^{-1}, 0.05 mg L^{-1} after reaction, respectively. Less Fe^{2+} was detected under higher pH, leading to the lower production of reactive species. Second, the elevation of pH$_0$ (pH$_0$ > 4) would benefit the precipitation of Fe(OH)$_3$,[38] inhibiting the availability of catalytic sites on the surface of nZVI.[39] Third, $^{\bullet}$OH has a higher oxidation potential at a lower pH, which was 2.65–2.80 V at pH 3.0 and 1.90 V at pH 7.0.[40] Therefore, acid condition was preferred to BPA degradation in the nZVI/SPC system.

3.3 Effect of water matrix on BPA degradation

Inorganic anions such as Cl$^-$, HPO$_4^{2-}$, NO$_3^-$ and NO$_2^-$ inherently exist in surface and ground water, which might react with free radicals and play an inhibited impact on contaminant degradation in AOPs.[13,41,42] In this study, BPA removal by adding different content of Cl$^-$, HPO$_4^{2-}$, NO$_3^-$ and NO$_2^-$ into nZVI/SPC system was discussed separately. As depicted in Fig. 6a, Cl$^-$ at the level of 1–10 mM showed inhibitory effect on BPA removal. It was probably because Cl$^-$ could compete with BPA to consume $^{\bullet}$OH to form Cl$_2$ and HOCl with weak oxidation
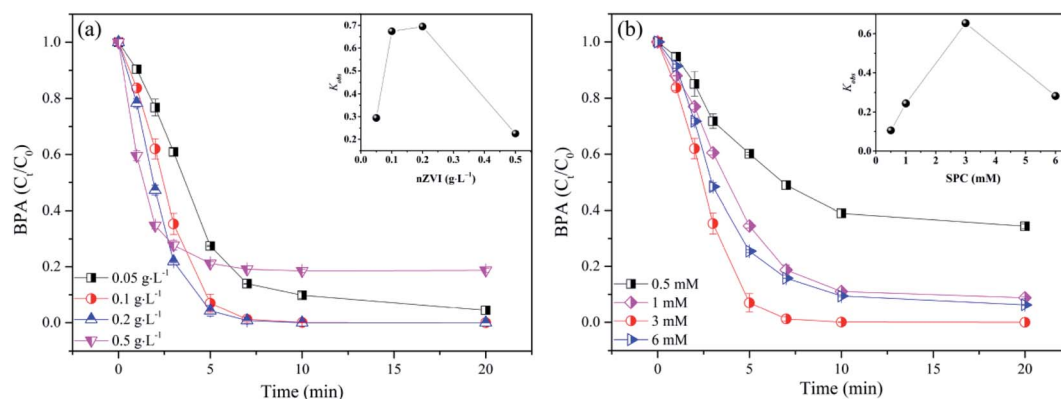

Fig. 4 Influence of nZVI loading (a) and SPC dosing (b) on BPA degradation in nZVI/SPC system: [BPA]$_0$ = 0.1 mM, [nZVI]$_0$ = 0.1 g L^{-1}, [SPC]$_0$ = 3 mM, pH$_0$ = 4.0.
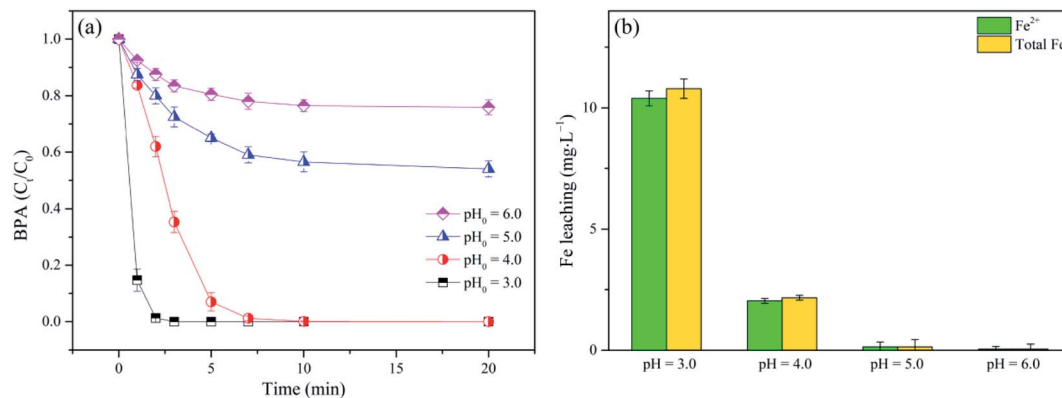
Fig. 5   (a) Effect of pH_0 on BPA degradation; (b) Fe leaching in the nZVI/SPC system. General reaction conditions: $[BPA]_0 = 0.1$ mM, $[nZVI]_0 = 0.1$ g L^{-1}, $[SPC]_0 = 3$ mM.
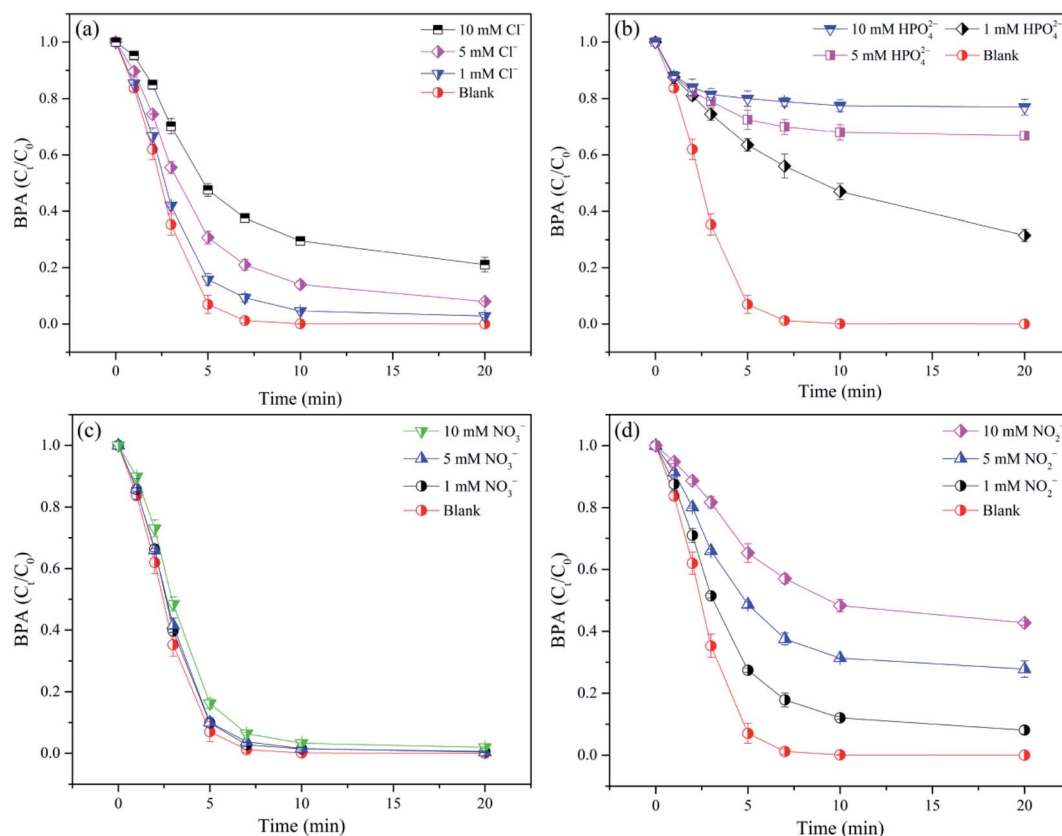

Fig. 6   Effect of anions on BPA degradation in nZVI/SPC system. (a) Cl^-; (b) HPO_4^{2-}; (c) NO_3^-; (d) NO_2^-. React conditions: $[BPA]_0 = 0.1$ mM, $[nZVI]_0 = 0.1$ g L^{-1}, $[SPC]_0 = 3$ mM, $pH_0 = 4.0$.

capacity.[43] Similarly, Fig. 6b showed that HPO_4^{2-} exhibited significant negative influence on BPA degradation. With the increase of HPO_4^{2-} concentration from 1.0 to 5.0 and 10.0 mM, BPA removal decreased from 68.5% to 33.2% and 23.0%, respectively. HPO_4^{2-} would complex with Fe^{2+} to block the active sites on the nZVI surface and suppress the released Fe^{2+}, which might inhibit ·OH generation.[6] Additionally, the presence of HPO_4^{2-}, as one of ·OH scavengers, could consume ·OH by the following reaction (eqn (12)).[6]

$$HPO_4^{2-} + ·OH \rightarrow HPO_4^{·-} + OH^- \qquad (12)$$
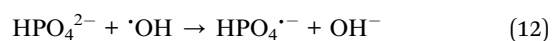
In case of NO_3^-, BPA degradation was slightly inhibited by the addition of 1, 5, and 10 mM NO_3^- (Fig. 6c), because NO_3^- was unable to complex with Fe^{2+} or Fe^{3+}, and also non-reactive to ·OH.[13] Conversely, a strong inhibitory effect on BPA removal was observed in the presence of NO_2^- (Fig. 6d). This phenomenon could be attributed to the scavenging reaction between
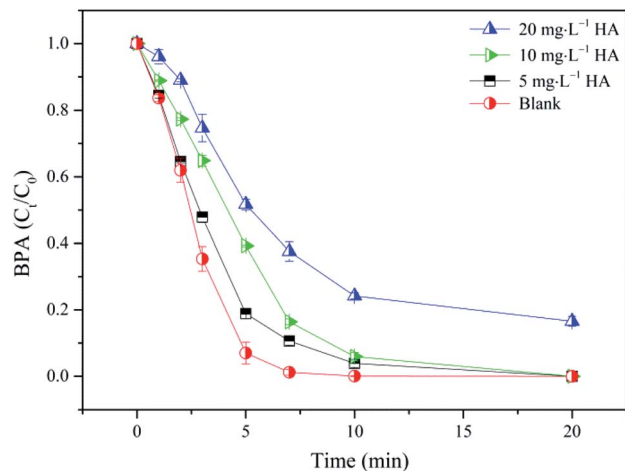
Fig. 7 Effect of HA on BPA degradation in the nZVI/SPC system: $[BPA]_0$ = 0.1 mM, $[nZVI]_0$ = 0.1 g L^{-1}, [SPC]$_0$ = 3 mM, pH_0 = 4.0.
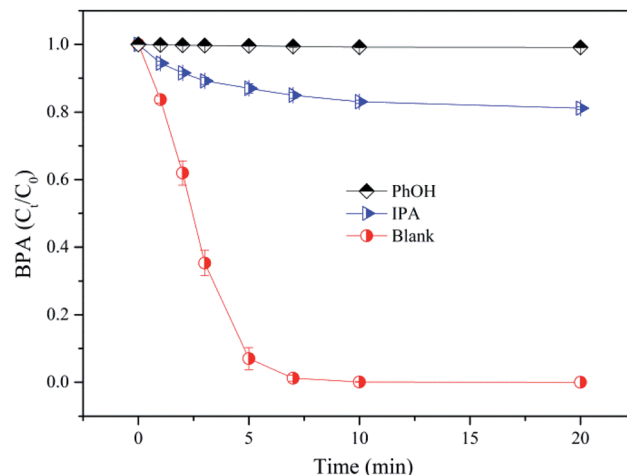

Fig. 8 The effects of IPA and PhOH on BPA degradation in nZVI/SPC system. General reaction conditions: $[BPA]_0$ = 0.1 mM, $[nZVI]_0$ = 0.1 g L^{-1}, [SPC]$_0$ = 3 mM, pH_0 = 4.0.

NO_2^- and $^\bullet OH$ ($k_{NO2^-, ^\bullet OH}$ = 1.2 × 10^{10} M^{-1} s^{-1}), leading to the generation of $NO_2^\bullet NO_2^\bullet$ with low oxidation potential.[44,45]

In addition, natural organic matters (NOMs), the common substances in water bodies, should be considered to investigate the influence on BPA removal in the nZVI/SPC process. Therefore, humic acid (HA), as a kind of representative NOMs, was selected to explore the effect of NOMs on BPA degradation. As shown in Fig. 7, when HA concentration increased to 5 mg L^{-1} and 10 mg L^{-1}, respectively, BPA removal rate was slightly inhibited. With the further increase of HA concentration to 20 mg L^{-1}, BPA removal efficiency still reached to 83% at 20 min. HA had the ability to consume a certain amount of $^\bullet OH$, and compete with target compounds, leading to the lower efficiency in AOPs.[36,46] These results indicated that the nZVI/SPC system has potential to resist appropriate amount of NOM interference on BPA degradation.

3.4 Identification of reactive species

As mentioned in previous literatures, $^\bullet OH$, $O_2^{\bullet-}$ and $CO_3^{\bullet-}$ were expected in the SPC system.[16,17,36] In this work, isopropanol (IPA) was used to study the existence of $^\bullet OH$, because it has a high reaction rate with $^\bullet OH$ ($k_{IPA, ^\bullet OH}$ = 3.9 × 10^9 M^{-1} s^{-1}) and a low reaction rate with $O_2^{\bullet-}$ ($k_{IPA, O_2^{\bullet-}}$ = 1 × 10^6 M^{-1} s^{-1}) and $CO_3^{\bullet-}$ ($k_{IPA, CO_3^{\bullet-}}$ = 4 × 10^4 M^{-1} s^{-1}).[47–49] Meanwhile, Phenol (PhOH) was employed as $^\bullet OH$ and $CO_3^{\bullet-}$ scavenger, which reacts rapidly with $^\bullet OH$ ($k_{PhOH, ^\bullet OH}$ = 6 × 10^8 M^{-1} s^{-1}) and $CO_3^{\bullet-}$ ($k_{PhOH, CO_3^{\bullet-}}$ = 1.2 × 10^9 M^{-1} s^{-1}),[16,50] and slowly with $O_2^{\bullet-}$ ($k_{PhOH, O_2^{\bullet-}}$ = 5.8 × 10^2 M^{-1} s^{-1}).[51] BPA degradation performance in the absence and presence of quenching agents was presented in Fig. 8. Both IPA and PhOH could prevent BPA removal in the nZVI/SPC system, and the inhibitory effect of PhOH was more significant. Specifically, in the absence of IPA or PhOH, BPA could be completely degraded in 10 min, whereas BPA removal rate decreased to 18.8% and 0.9% with the addition of 30 mM IPA and PhOH, respectively. This result implied that both $^\bullet OH$ and $CO_3^{\bullet-}$ participated in the degradation of BPA, and $^\bullet OH$ was the main reactive oxygen radical for BPA removal in nZVI/SPC

system. But the contribution of $O_2^{\bullet-}$ was negligible. This is due to the fact that HCO_3^- can scavenge $O_2^{\bullet-}$ to be $CO_3^{\bullet-}$, which selectively react with electron-rich compounds, like phenols.[50,52]

3.5 Mechanistic insight of the nZVI/SPC system

As presented in Fig. 9, the XRD patterns of nZVI before use were corresponded to the standard peaks of Fe^0 (JCPDS no. 36-0696).[53] After 20 min reaction, the new peaks at 26.6°, 35.6° and 60.6° are observed in used nZVI, which are relevant to the crystalline structures of Fe_3O_4 (JCPDS no. 89-6466), FeO (JCPDS no. 89-0690) and FeOOH (JCPDS no. 70-0410), respectively. These results suggested that iron oxides and oxide-hydroxides were formed on the surface of nZVI during the activation of SPC.

To better understand the roles of Fe and O species on the nZVI surface in SPC activation, the XPS spectra of nZVI before
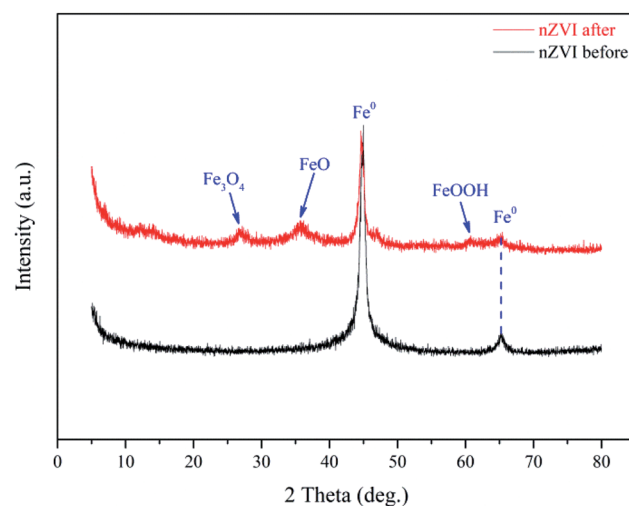

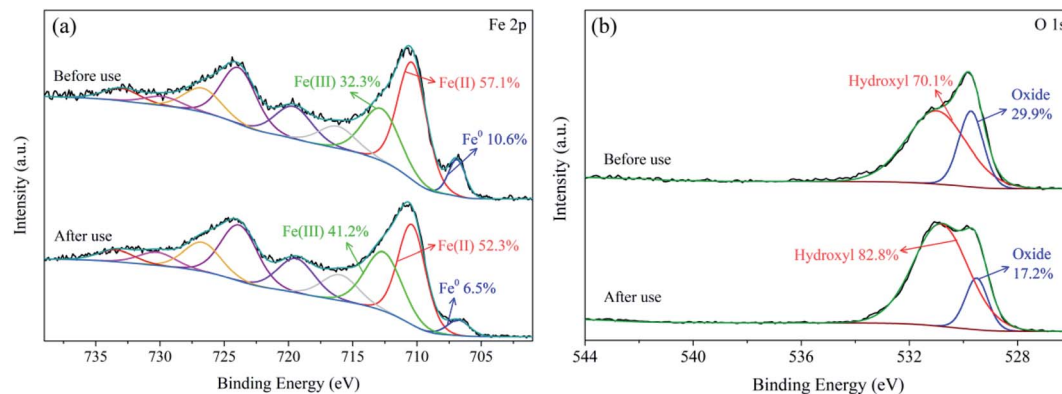**Fig. 9** XRD of nZVI before and after use.

Fig. 10 XPS spectra on Fe 2p (a) and O 1s (b) of nZVI catalyst before and after use.

and after reactions were recorded. As illustrated in Fig. 10a, the peaks of Fe $2p_{3/2}$ at 706.8 eV, 710.3 eV, and 712.7 eV indicated the existence of Fe^0, Fe_3O_4 and FeOOH on the nZVI surface before reaction, respectively.[21,53–55] Based on the Fe $2p_{3/2}$ spectrum, the Fe^0, Fe(II) and Fe(III) content of the nZVI before use were 10.6%, 57.1% and 23.3%, but account for 6.5%, 52.3% and 41.2% for the nZVI after use, respectively. After the reactions, the decrease of Fe^0 and Fe(II) indicated that electron transfer occurred on the nZVI surface and Fe^{2+} was released from the catalyst,[20] resulting in the increase of Fe(III) fraction and $^•OH$ production, according to the eqn (4).

In addition, the O 1s spectrum is shown in Fig. 10b. The two main peaks at 529.7 eV and 531.0 eV were assigned to iron oxide and surface hydroxyl species before reaction, correspondingly.[53,55] After reactions, with the decrease of the fraction of iron oxide, an iron hydroxide layer was formed, making the composition of surface hydroxyl species increased. The results further proved that the formation of iron oxides was the important step in activating SPC by nZVI.

Overall, based on the above analysis, the chemical reaction mechanism between nZVI and SPC was proposed as shown in Fig. 11. First, nZVI was corroded to generate Fe(II)-contained oxides on the surface and Fe^{2+} ions that leached into the reaction solution (eqn (4) and (5)). Then, Fe^{2+} ions could activate H_2O_2 directly, generated from SPC, to engender $^•OH$ and Fe^{3+}. The formed Fe^{3+} would be transformed to Fe(III)-contained

oxides, deposited on the surface of nZVI.[53] On the other hand, Fe^{2+} could be regenerated from the reduction of Fe^{3+},[34,48] further promoting the activation of SPC. In addition, CO_3^{2-} and HCO_3^-, as by-products of SPC decomposition, could transform to be $CO_3^{•-}$ through the reaction with $^•OH$ as shown in eqn (2) and (3). Finally, BPA was degraded to TPs by $^•OH$ and $CO_3^{•-}$ *via* direct radical attachment and electron transfer, respectively.

3.6 BPA degradation pathways

In this study, the TPs of BPA in the nZVI/SPC system were identified by LC-MS. Four compounds were detected with identified m/z values, namely B1 (monohydroxylated BPA, $m/z = 243.101$), B2 (dihydroxylated BPA, $m/z = 259.096$), B3 (*p*-isopropylphenol, $m/z = 151.075$) and B4 (1-(2,4-dihydroxyphenyl) ethan-1-one, $m/z = 151.038$). Detailed information was supplied in ESI.† The possible degradation pathway of BPA (Fig. 12) was proposed based on the monitored TPs and the
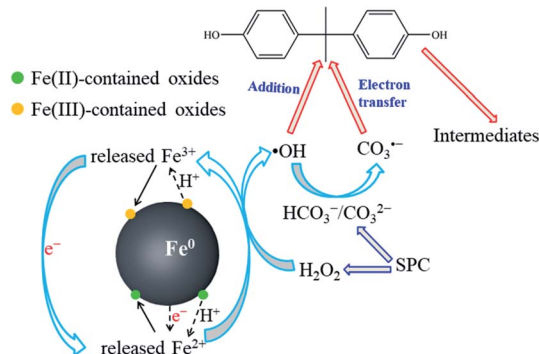

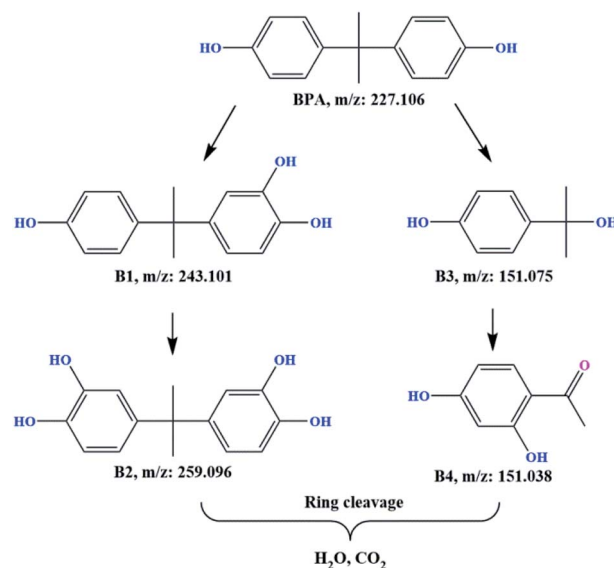Fig. 11 Proposed mechanism of BPA degradation in the nZVI/SPC system.

Fig. 12 Possible degradation pathway of BPA in the nZVI/SPC system. Reaction conditions: $[BPA]_0 = 0.1$ mM, $[nZVI]_0 = 0.1$ g L^{-1}, $[SPC]_0 = 3$ mM, $pH_0 = 4.0$.
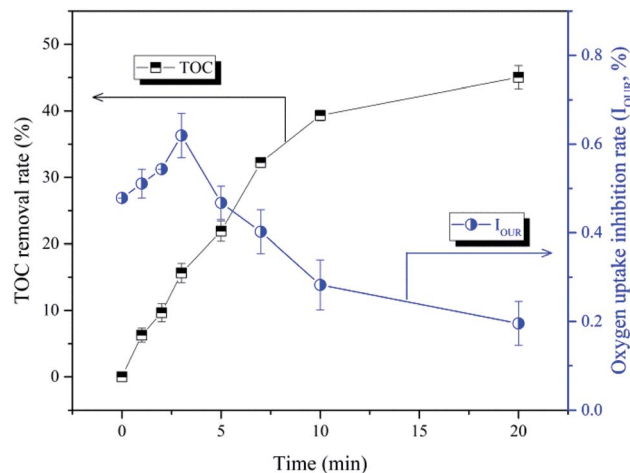
Fig. 13 Changes of TOC and bio-toxicity during BPA treatment in the nZVI/SPC system. Reaction conditions: $[BPA]_0 = 0.1$ mM, $[nZVI]_0 = 0.1$ g L^{-1}, $[SPC]_0 = 3$ mM, $pH_0 = 4.0$.

previous studies.[56,57] First, $\cdot OH$ might attack the aromatic ring of BPA through hydroxylation to produce B1, and further hydroxylation to be B2. On the other hand, BPA could be converted into phenolic-BPA radical cation under the attack of $CO_3^{\cdot-}$ by capturing electrons.[16] After further interacted with water, hydroxybenzene TPs (B1) was generated. Then, B1 was hydroxylation into B2 following the same mechanism.[16] Second, $\cdot OH$ could attack the electron-rich alkyl carbon of BPA to remove a benzene ring, resulting in the formation of alkyl hydroxylation product (B3). Subsequently, B3 was gradually converted to B4 with further oxidized by $\cdot OH$. At last, these BPA TPs would be transformed to the ring-cleavage products *via* hydroxylation and oxidation,[58] and be further mineralized into CO_2 and H_2O.

3.7 Mineralization and toxicity assessment during BPA degradation

The mineralization efficiency of BPA in the nZVI/SPC system was assessed through monitoring the change of TOC. As illustrated in Fig. 13, BPA mineralization rate was continuously increased along with the decomposition of BPA. After 20 min, 45.0% of the TOC was removed under the optimized reaction conditions, which implied that BPA was gradually transformed into smaller molecules. However, the bio-toxicity of BPA and TPs showed a different trend compared to the TOC result. The oxygen uptake inhibition rate increased from 47.8% to 62.0% in the first 3 min of reaction, and gradually decreased to 19.6% in the remaining reaction time (3–20 min). Some TPs that were generated during the initial reaction stage (0–3 min) caused higher bio-toxicity than the parent compound, such as B3 and B4.[3,59] These toxic TPs were finally disassembled and mineralized to low or non-toxic products in the nZVI/SPC system.

4. Conclusions

In this study, the catalytic efficiency of nZVI particles in activating SPC to remove BPA was investigated for wastewater

treatment. BPA degradation efficiency was enhanced with increased nZVI loading and SPC dosing in the adequate range at low initial pH. Furthermore, the Cl^-, HPO_4^{2-}, NO_2^- anions and HA in aqueous solution inhibited BPA removal in the selected range. In the nZVI/SPC system, $\cdot OH$ was the dominant active species, while $CO_3^{\cdot-}$ slightly contributed to the degradation of BPA. In addition, surface corrosion, Fe^{2+} releasing, and iron species conversion play significant roles in the activation of SPC by nZVI. The possible degradation pathways of BPA were proposed based on the TPs detected by LC-MS. This work supports that the nZVI/SPC system can be used as an efficient, cost effective, and environmental-friendly technology for the remediation of BPA in wastewater treatment, owing to its high catalytic activity, good reusability, and treatment safety.

Conflicts of interest

The authors declare no conflict of interest.

Acknowledgements

References

1 Y. Xie, P. Li, Y. Zeng, X. Li, Y. Xiao, Y. Wang and Y. Zhang, *Chem. Eng. J.*, 2018, **335**, 728–736.

2 Y. Wang, S. Zhao, W. Fan, Y. Tian and X. Zhao, *Environ. Sci.: Nano*, 2018, **5**, 1933–1942.

3 J. Deng, M. Xu, C. Qiu, Y. Chen, X. Ma, N. Gao and X. Li, *Appl. Surf. Sci.*, 2018, **459**, 138–147.

4 J. Liu, L. Zhang, G. Lu, R. Jiang, Z. Yan and Y. Li, *Ecotoxicol. Environ. Saf.*, 2021, **208**, 111481.

5 S. Yang, P. Wu, J. Liu, M. Chen, Z. Ahmed and N. Zhu, *Chem. Eng. J.*, 2018, **350**, 484–495.

6 L. Liu, X. Xu, Y. Li, R. Su, Q. Li, W. Zhou, B. Gao and Q. Yue, *Chem. Eng. J.*, 2020, **382**, 122780.

7 X. Xu, S. Zong, W. Chen and D. Liu, *Chem. Eng. J.*, 2019, **369**, 470–479.

8 J. Sharma, I. M. Mishra, D. D. Dionysiou and V. Kumar, *Chem. Eng. J.*, 2015, **276**, 193–204.

9 M. Chen, Z. Zhang, L. Zhu, N. Wang and H. Tang, *Chem. Eng. J.*, 2019, **361**, 1190–1197.

10 N. Wang, Q. Hu, X. Du, H. Xu and L. Hao, *Adv. Powder Technol.*, 2019, **30**, 2369–2378.

11 N. Wang, X. Sun, Q. Zhao and P. Wang, *Chem. Eng. J.*, 2021, **406**, 126734.

12 A. Mirzaei, Z. Chen, F. Haghighat and L. Yerushalmi, *Chemosphere*, 2017, **174**, 665–688.

13 M. M. Sablas, M. D. G. de Luna, S. Garcia-Segura, C.-W. Chen, C.-F. Chen and C.-D. Dong, *Sep. Purif. Technol.*, 2020, **250**, 117269.

14 Y. Li, Y. Zhu, D. Wang, G. Yang, L. Pan, Q. Wang, B.-J. Ni, H. Li, X. Yuan, L. Jiang and W. Tang, *Water Res.*, 2020, **174**, 115626.

15 Z. Miao, X. Gu, S. Lu, M. L. Brusseau, N. Yan, Z. Qiu and Q. Sui, *J. Hazard. Mater.*, 2015, **300**, 530–537.

16 J. Gao, X. Duan, K. O'Shea and D. D. Dionysiou, *Water Res.*, 2020, **171**, 115394.

17 Y. Huang, M. Kong, D. Westerman, E. G. Xu, S. Coffin, K. H. Cochran, Y. Liu, S. D. Richardson, D. Schlenk and D. D. Dionysiou, *Environ. Sci. Technol.*, 2018, **52**, 12697–12707.

18 Z. W. Miao, X. G. Gu, S. G. Lu, X. K. Zang, X. L. Wu, M. H. Xu, L. B. B. Ndong, Z. F. Qiu, Q. Sui and G. Y. Fu, *Chemosphere*, 2015, **119**, 1120–1125.

19 S. Sajjadi, A. Khataee, R. Darvishi Cheshmeh Soltani, N. Bagheri, A. Karimi and A. Ebadi Fard Azar, *J. Ind. Eng. Chem.*, 2018, **68**, 406–415.

20 C. Kim, J.-Y. Ahn, T. Y. Kim, W. S. Shin and I. Hwang, *Environ. Sci. Technol.*, 2018, **52**, 3625–3633.

21 J. Cao, L. Lai, B. Lai, G. Yao, X. Chen and L. Song, *Chem. Eng. J.*, 2019, **364**, 45–56.

22 H. Dong, K. Hou, W. Qiao, Y. Cheng, L. Zhang, B. Wang, L. Li, Y. Wang, Q. Ning and G. Zeng, *Chem. Eng. J.*, 2019, **359**, 1046–1055.

23 R. Chen, H. Yin, H. Peng, X. Wei, X. Yu, D. Xie, G. Lu and Z. Dang, *Environ. Pollut.*, 2020, **260**, 113983.

24 W. Zhang, H. Gao, J. He, P. Yang, D. Wang, T. Ma, H. Xia and X. Xu, *Sep. Purif. Technol.*, 2017, **172**, 158–167.

25 R. Cheng, C. Cheng, G.-h. Liu, X. Zheng, G. Li and J. Li, *Chemosphere*, 2015, **141**, 138–143.

26 A. Liu, J. Liu, J. Han and W.-x. Zhang, *J. Hazard. Mater.*, 2017, **322**(part A), 129–135.

27 J. Du, J. Bao, C. Lu and D. Werner, *Water Res.*, 2016, **102**, 73–81.

28 J. Du, J. Bao, Y. Liu, H. Ling, H. Zheng, S. H. Kim and D. D. Dionysiou, *J. Hazard. Mater.*, 2016, **320**, 150–159.

29 Y. M. Yoon, P. Westerhoff, S. A. Snyder and M. Esparza, *Water Res.*, 2003, **37**, 3530–3537.

30 M. L. Dell'Arciprete, J. M. Soler, L. Santos-Juanes, A. Arques, D. O. Mártire, J. P. Furlong and M. C. Gonzalez, *Water Res.*, 2012, **46**, 3479–3489.

31 H. Liu, J. Yao, L. Wang, X. Wang, R. Qu and Z. Wang, *Chem. Eng. J.*, 2019, **358**, 1479–1488.

32 W. Jiang, D. D. Dionysiou, M. Kong, Z. Liu, Q. Sui and S. Lyu, *Chem. Eng. J.*, 2020, **380**, 122537.

33 J. A. Donadelli, L. Carlos, A. Arques and F. S. García Einschlag, *Appl. Catal., B*, 2018, **231**, 51–61.

34 L. Wang, J. Yang, Y. Li, J. Lv and J. Zou, *Chem. Eng. J.*, 2016, **284**, 1058–1067.

35 M. Danish, X. Gu, S. Lu, A. Ahmad, M. Naqvi, U. Farooq, X. Zhang, X. Fu, Z. Miao and Y. Xue, *Chem. Eng. J.*, 2017, **308**, 396–407.

36 H. Cui, X. Gu, S. Lu, X. Fu, X. Zhang, G. Y. Fu, Z. Qiu and Q. Sui, *Chem. Eng. J.*, 2017, **309**, 80–88.

37 I. Hussain, M. Y. Li, Y. Q. Zhang, Y. C. Li, S. B. Huang, X. D. Du, G. Q. Liu, W. Hayat and N. Anwar, *Chem. Eng. J.*, 2017, **311**, 163–172.

38 M. Danish, X. G. Gu, S. G. Lu, M. H. Xu, X. Zhang, X. R. Fu, Y. F. Xue, Z. W. Miao, M. Naqvi and M. Nasir, *Res. Chem. Intermed.*, 2016, **42**, 6959–6973.

39 R. Li, X. Jin, M. Megharaj, R. Naidu and Z. Chen, *Chem. Eng. J.*, 2015, **264**, 587–594.

40 A. A. Burbano, D. D. Dionysiou, M. T. Suidan and T. L. Richardson, *Water Res.*, 2005, **39**, 107–118.

41 X. Y. Yu and J. R. Barker, *J. Phys. Chem. A*, 2003, **107**, 1313–1324.

42 X. Y. Lou, L. X. Wu, Y. G. Guo, C. C. Chen, Z. H. Wang, D. X. Xiao, C. L. Fang, J. S. Liu, J. C. Zhao and S. Y. Lu, *Chemosphere*, 2014, **117**, 582–585.

43 Y. Yang, J. J. Pignatello, J. Ma and W. A. Mitch, *Environ. Sci. Technol.*, 2014, **48**, 2344–2351.

44 C. Chen, Z. Wu, S. Zheng, L. Wang, X. Niu and J. Fang, *Environ. Sci. Technol.*, 2020, **54**, 8455–8463.

45 J. Li, M. Xu, G. Yao and B. Lai, *Chem. Eng. J.*, 2018, **348**, 1012–1024.

46 X. Fu, X. Gu, S. Lu, Z. Miao, M. Xu, X. Zhang, Z. Qiu and Q. Sui, *Chem. Eng. J.*, 2015, **267**, 25–33.

47 P. Yan, Q. Sui, S. Lyu, H. Hao, H. F. Schröder and W. Gebhardt, *Sci. Total Environ.*, 2018, **640–641**, 973–980.

48 X. Fu, X. Gu, S. Lu, V. K. Sharma, M. L. Brusseau, Y. Xue, M. Danish, G. Y. Fu, Z. Qiu and Q. Sui, *Chem. Eng. J.*, 2017, **309**, 22–29.

49 T. Liu, K. Yin, C. Liu, J. Luo, J. Crittenden, W. Zhang, S. Luo, Q. He, Y. Deng, H. Liu and D. Zhang, *Water Res.*, 2018, **147**, 204–213.

50 T. Zhao, P. Li, C. Tai, J. She, Y. Yin, Y. a. Qi and G. Zhang, *J. Hazard. Mater.*, 2018, **346**, 42–51.

51 Y. Tsujimoto, H. Hashizume and M. Yamazaki, *Int. J. Biochem.*, 1993, **25**, 491–494.

52 Y. Liu, X. He, X. Duan, Y. Fu, D. Fatta-Kassinos and D. D. Dionysiou, *Water Res.*, 2016, **95**, 195–204.

53 C. Tan, Y. Dong, D. Fu, N. Gao, J. Ma and X. Liu, *Chem. Eng. J.*, 2018, **334**, 1006–1015.

54 J. Wu, B. Wang, L. Blaney, G. Peng, P. Chen, Y. Cui, S. Deng, Y. Wang, J. Huang and G. Yu, *Chem. Eng. J.*, 2019, **361**, 99–108.

55 C. Ding, S. Xiao, S. Lin, P. Yu, M.-e. Zhong, L. Yang, H. Wang, L. Su, C. Liao, Y. Zhou, Y. Deng and D. Gong, *Chem. Eng. J.*, 2019, **360**, 104–114.

56 R. A. Torres, F. Abdelmalek, E. Combet, C. Petrier and C. Pulgarin, *J. Hazard. Mater.*, 2007, **146**, 546–551.

57 X. Li, Z. H. Wang, B. Zhang, A. I. Rykov, M. A. Ahmed and J. H. Wang, *Appl. Catal., B*, 2016, **181**, 788–799.

58 Z. Dong, Q. Zhang, B.-Y. Chen and J. Hong, *Chem. Eng. J.*, 2019, **357**, 337–347.

59 R. Mtibaà, D. R. Olicón-Hernández, C. Pozo, M. Nasri, T. Mechichi, J. González and E. Aranda, *Ecotoxicol. Environ. Saf.*, 2018, **156**, 87–96.